AGU PUBLICATIONS

JGR

Journal of Geophysical Research: Oceans

RESEARCH ARTICLE

10.1002/2015JC011571

Special Section:
Physical Processes Responsible for Material Transport in the Gulf of Mexico for Oil Spill Applications

Modeling the influence of deep water application of dispersants on the surface expression of oil: A sensitivity study

Jeremy M. Testa[1], E. Eric Adams[2], Elizabeth W. North[3], and Ruoying He[4]

[1]Chesapeake Biological Laboratory, University of Maryland Center for Environmental Science, Solomons, Maryland, USA, [2]Department of Civil and Environmental Engineering, Massachusetts Institute of Technology, Cambridge, Massachusetts, USA, [3]Horn Point Laboratory, University of Maryland Center for Environmental Science, Cambridge, Maryland, USA, [4]Department of Marine, Earth, and Atmospheric Sciences, North Carolina State University, Raleigh, North Carolina, USA

Abstract Although the effects of chemical dispersants on oil droplet sizes and ascent speeds are well-known, the fate and transport of dispersed oil droplets of different sizes under varying hydrodynamic conditions can be difficult to assess with observations alone. We used a particle tracking model to evaluate the effect of changes in droplet sizes due to dispersant application on the short-term transport and surface expression of oil released under conditions similar to those following the 3 June 2010 riser cutting during the Deepwater Horizon event. We used simulated injections of oil droplets of varying size and number under conditions associated with no dispersant application and with dispersant application at 50% and 100% efficiency. Due to larger droplet sizes in the no-dispersant scenario, all of the simulated oil reached the surface within 7 h, while only 61% and 28% of the oil reached the surface after 12 h in the 50% and 100% dispersant efficiency cases, respectively. The length of the surface slick after 6 h was ~2 km in the no-dispersant case whereas there was no surface slick after 6 h in the 100% dispersant case, because the smaller oil droplets which resulted from dispersant application had not yet reached the surface. Model results suggest that the application of dispersants at the well head had the following effects: (1) less oil reached the surface in the 6-12 h after application, (2) oil had a longer residence time in the water-column, and (3) oil was more highly influenced by subsurface transport.

Key Points:
- Numerical models are useful for examining the sensitivity of oil fate and transport to dispersant application
- Simulated dispersant application strongly influenced the timing and spatial extent of surfacing oil
- Simulated dispersant application resulted in slower oil surfacing time and higher subsurface retention

Correspondence to:
J. Testa,
jtesta@umces.edu

Citation:
Testa, J. M., E. Eric Adams, E. W. North, and R. He (2016), Modeling the influence of deep water application of dispersants on the surface expression of oil: A sensitivity study, *J. Geophys. Res. Oceans*, *121*, 5995–6008, doi:10.1002/2015JC011571.

Received 15 DEC 2015
Accepted 4 JUL 2016
Accepted article online 6 JUL 2016
Published online 19 AUG 2016

1. Introduction

The Deepwater Horizon oil spill was the largest accidental spill on record, occurred deep in the Gulf of Mexico (~1.5 km), and was among the few spills during which chemical dispersants were applied in the subsurface. The depth of the spill, and the many physical, chemical and biological processes that affect hydrocarbons after release, has made it challenging to understand the mass flow of hydrocarbons along different transport pathways, with significant sources of uncertainty remaining despite integrated and rigorous efforts [*Ryerson et al.*, 2011, 2012]. In addition, the unique application of chemical dispersants at the well head further complicated partitioning the surfacing component of liquid hydrocarbons. The objective of this research was to examine the influence of dispersant application at the well head on the timing, mass, and spatial extent of the liquid hydrocarbon plume as it reached the surface.

Although a large fraction of the hydrocarbons originating from the Deepwater Horizon spill were found in deep, subsurface intrusions [*Ryerson et al.*, 2012; *Socolofsky et al.*, 2011], a substantial amount of oil reached the surface (~13% of the total hydrocarbon mass escaping the cap) in a surfacing zone that was ~1.6 km in diameter [*Ryerson et al.*, 2012]. When a spill occurs deep below the surface, a rising oil plume develops in the vicinity of the well head and eventually entrains enough seawater to reach a buoyancy comparable to the ambient fluid [*NRC*, 2003]. As a result, hydrocarbons may be found in horizontal intrusions in deep water depending on the current velocity, degree of stratification, and properties of the hydrocarbons released during the spill [*Socolofsky et al.*, 2011]. Despite the formation of these intrusions, larger, buoyant oil droplets continue to rise, forming the surface slicks observed during subsurface oil spills [e.g., *Ryerson et al.*, 2012]. The horizontal displacement of the rising oil is largely influenced by ambient current velocities (which can vary greatly with depth) and the associated residence time of oil droplets; this residence time scales to droplet size via nonlinear relationships between droplet size and rise velocity [*Zheng and Yapa*, 2000]. During the Deepwater Horizon spill, it is likely that oil droplets with millimeter-scale diameters transported

most of the mass of the oil that surfaced based on measurements of current velocities above the well head and the fact that observers on response vessels reported a ~3 h lag in changes in the characteristics of the surfacing slick after a deliberate intervention at the well head [*Ryerson et al*., 2012].

Predicting the transport of oil released during the Deepwater Horizon spill was further complicated by the injection of chemical dispersants at the well head. During the spill, 2,900,000 L of chemical dispersant were injected into the hydrocarbon plume near the seafloor, the largest application of this type of chemical dispersal attempted at the time [*Kujawinski et al*., 2011]. These dispersants, which include both surfactants and hydrocarbon-based solvents (e.g., Corexit 9500A) [*Place et al*., 2010], were intended to reduce the interfacial tension between oil and water and thus reduce the size of the oil droplets [*Brandvik et al*., 2013a]. The application of these compounds therefore would have reduced the size of oil droplets, influenced the rise velocity of treated oil, changed the volume of oil that reached the surface, and correspondingly, affected the volume of oil that was retained in the subsurface to be transported horizontally or degraded by the microbial community. Although these effects have been simulated using parameterizations from the Deepspill experiments [*Yapa et al*., 2012], the influence of the change in droplet size due to dispersant application on the short-term transport of oil has not yet been quantified using parameterizations from the Deepwater Horizon spill. In addition, the dispersant treatments during the Deepwater Horizon spill were not 100% efficient (i.e., they did not treat every oil droplet released [*Dehkharghanian and Socolofsky*, 2014]). Therefore a modeling sensitivity study could help increase understanding of the effect of dispersant application with different efficiencies on the subsequent transport and surfacing of oil.

Lagrangian particle tracking models are an important component of oil spill response models (e.g., GNOME [*Zelenke et al*., 2012], CDOG [*Zheng et al*., 2003], OILTRANS [*Berry et al*., 2012]) and are increasing being applied as experimental tools to better understand the processes that influence the transport of hydrocarbons from deep water spills. Lagrangian models have demonstrated the importance of bathymetric steering [*Weisberg et al*., 2011] and small-scale eddies [*Chang et al*., 2011] on the transport of subsurface plumes. In addition, Lagrangian models applied in the far-field (when oil droplet buoyancy and ambient conditions dominate transport) indicate that the mass and distance of transport of oil in the subsurface is strongly influenced by the initial droplet size and biodegradation rates within the water column [*Lindo-Atichati et al*., 2014; *Mariano et al*., 2011; *North et al*., 2011, 2015; *Paris et al*., 2012]. Lagrangian models have also been applied in the near-field (when jet/plume dynamics dominate transport) and demonstrate that plumes of very small oil droplets (less than 500 μm) can form and persist in the subsurface [*Yapa et al*., 2012]. In addition to providing information on oil droplet dispersal, Lagrangian models can be used to quantify the sensitivity of transport predictions to different components of water motion (e.g., advection and diffusion) as well as the characteristics of oil droplets (e.g., ascent speed, dissolution) to better understand which factors are most influential and therefor important to parameterize accurately in response models.

The purpose of this analysis was to estimate the effects of subsurface dispersant application on droplet sizes and the subsequent change in the timing, mass and spatial extent of oil droplets as they reached the surface during the Deepwater Horizon oil spill, and to better understand the role of advection, diffusion, and droplet size on the predictions of the surfacing oil. To do so, a semiempirical near-field model was coupled with a Lagrangian particle tracking model to track the movement of individual oil droplets over a 36 h period following the cut of the riser on 3 June 2010. Two fundamental questions guided this research: (1) How does the effect of dispersants on droplet size influence the surface expression of oil?, and (2) How does the simulation of varying hydrodynamic conditions influence the predicted size and timing of the surfacing plume of oil? These questions are addressed using a series of model simulations under a range of hydrodynamic conditions and dispersant treatment scenarios.

A two-step approach was used to simulate the initial distribution, volume, release location, and eventual transport of oil droplets from an event similar to the Deepwater Horizon oil spill on 3 June 2010. First, a near-field model which included a series of semiempirical equations for oil droplet size, multiphase plume behavior in stratified water, and the behavior of different sized droplets within such multiphase plumes was used to estimate release locations and droplet size distributions. Second, a three-dimensional South Atlantic Bight and Gulf of Mexico (SABGOM) hydrodynamic model coupled with the Lagrangian TRANSport (LTRANS) particle tracking model were used to simulate oil droplet transport in the far-field after which near-field plume dynamics no longer influenced the transport of oil droplets (i.e., when droplet ascent was based on the diameter and density of oil droplets and circulation patterns alone).

2. Methods

2.1. Near-Field Model

The semiempirical, near-field model was used to calculate the initial conditions for three sets of simulations with (1) no dispersants, (2) dispersant application at the well-head with 50% efficiency and (3) dispersant application with 100% efficiency. The initial conditions included: the droplet size distribution, the height above bottom at which droplets exited the plume and entered the far-field model, and the horizontal spread of droplets at this depth.

2.1.1. Droplet Size Distribution

Johansen et al. [2013] predict the volume median droplet size d_{50} of oil jetted at high velocity (i.e., within the atomization range) as a function of a modified Weber number. For an oil-only release their relationship is

$$d_{50}/D = A\left(We/\left[1+BVi(d_{50}/D)^{1/3}\right]\right)^{-3/5} \quad (1)$$

where We is the Weber number defined as

$$We=\rho U^2 D/\gamma \quad (2)$$

and Vi is the Viscosity number defined as

$$Vi=\mu U/\gamma \quad (3)$$

In the above, d_{50}/D is the ratio of the median droplet size to diameter of the orifice, D and U are the diameter and exit velocity of the orifice, and γ, ρ and μ are the oil-water interfacial tension, the oil density, and dynamic viscosity, respectively, and A and B are empirical coefficients (Table 1). By calibrating against laboratory data reported by *Brandvik et al*. [2013a], *Johansen et al*. [2013] found A = 15 and B = 0.08. *Brandvik et al*. [2013b] later conducted similar tests and found A = 24.8 and B = 0.08. The latter pair of coefficients was used in this study.

For a discharge containing both oil and gas, the two studies argue that equation (1) can be applied if U is replaced with a "corrected" velocity that accounts for the increase in plume momentum (because the oil is discharged through a smaller cross section) and the increase in buoyancy (which leads to a further increase in momentum with distance along the trajectory). The corrected velocity is given by

$$U_C = U_n(1+Fr^{-1}) \quad (4)$$

where

$$U_n = U/(1-n)^{1/2} \quad (5)$$

and

$$Fr = U_n/(g[\rho_w-\rho(1-n)]/\rho_w D)^{1/2} \quad (6)$$

where ρ_w is the density of the receiving water and n is the void fraction associated with the gas.

Table 1 provides representative values of parameters that were used in equations (1–6) which represent conditions like those during the *Deepwater Horizon* spill. Data are from *Lehr et al*. [2010] and pertain to conditions after the riser was cut on 3 June 2010. Under these conditions the oil was directed upward through

Table 1. Parameters Used to Compute Volume Median Droplet Size (d_{50}) for the Deepwater Horizon Spill Oil Under Two Dispersant Scenarios (cgs Units)[a]

Treatment	ρ g cm^{-3}	D cm	U cm s^{-1}	n	Fr	U_C cm s^{-1}	γ g s^{-2}	μ g cm^{-1}s^{-1}	V_i	d_{50}/D	d_{50} cm	# Droplets Simulated
No Dispersant	0.85	49	65	0.55	0.6	272	23	0.041	0.48	0.021	1.03	1,205,820
Dispersant	0.85	49	65	0.55	0.6	272	0.11	0.041	96	0.0014	0.069	7,978,896

[a]D and U are the diameter and exit velocity of the orifice, γ, ρ and μ are the oil-water interfacial tension, the oil density, and dynamic viscosity, respectively. n is the void ration, Fr is the Froude number, U_C is the characteristic plume velocity, V_i is the viscosity number, and d_{50}/D is the ratio of the median droplet size to diameter of the orifice.

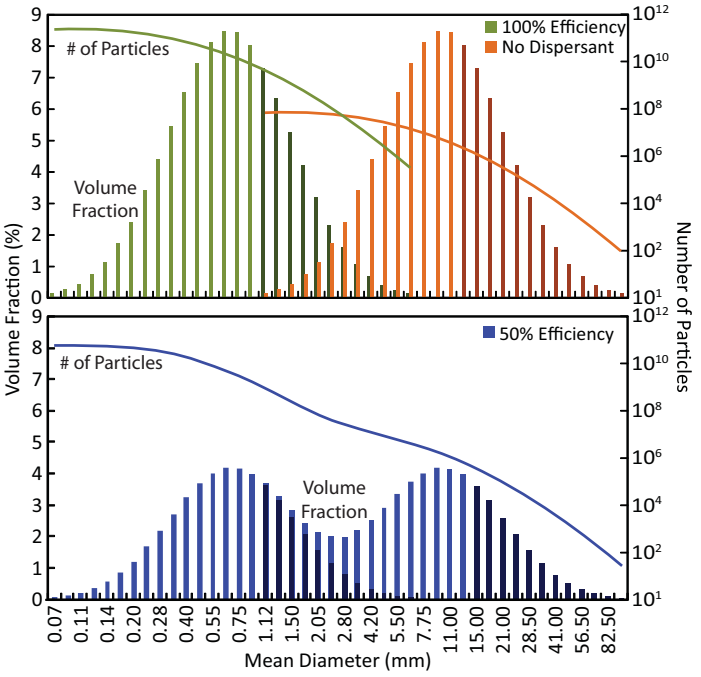

Figure 1. Distribution of volume fraction (bars) and oil droplet number (lines) in particle diameter size classes which were used to create initial droplet size distributions for simulations (top) without dispersants (orange) and with dispersants applied at the wellhead with (top) 100% efficiency (green) and (bottom) 50% efficiency (blue). Volume fraction distributions were based on experimental work [*Brandvik et al*., 2013a; *Johansen et al*., 2013]. Particle number was based on volume of oil released on 3 June 2010. The darker shaded bars in each simulation represent droplets predicted from the [*Johansen et al*., 2013] formulation whose size exceeds realistic stability given the interfacial tension [*Clift et al*., 1978]. The volume associated with these droplets was added to that for the largest stable droplet diameter (see methods).

an orifice of diameter 49 cm at a rate of 126,000 $cm^3\ s^{-1}$. The oil was accompanied by natural gas, as well as some seawater and possibly some hydrates. From a dynamic standpoint, the most important of these constituents is gas and calculations in Table 1 assume a gas flow rate characterized by a void ratio of n = 0.55. Without dispersant treatment the predicted value of d_{50} is 1.03 cm after the riser was cut. Similar calculations pertaining to the period before the riser was cut, where the oil flowed horizontally at a rate of about 103,000 $cm^3\ s^{-1}$ through a 35 cm diameter orifice gave a d_{50} of 0.77 cm. The "postriser cut" conditions were applied for this study and assume a single flow, although kinks in the riser allowed for additional flows during the spill.

Data from *Johansen et al*. [2013] suggest that the droplet distribution can be fit, approximately, by either a log-normal or Rosin-Rammler distribution. The log-normal provides an excellent fit at larger droplets sizes and a relatively poor fit at smaller droplet sizes, while the Rosin-Rammler distribution shows moderate discrepancy at both ends. For this study, the log-normal distribution was chosen because the objective of this study was to examine the surfacing expression of oil in large droplets of approximately millimeter-scale [*Ryerson et al*., 2012]. The log-normal distribution can be written

$$c\ (\ln\ d)\ =\ c\ (\ln\ d_{50})\ \exp[-([\ln\ [d/d_{50}]^2/2\sigma^2)] \tag{7}$$

where c (ln d_{50}) is the relative droplet volume density (concentration) of the peak droplet size d_{50}, c (ln d) is the relative droplet volume density (concentration) of droplets of diameter d, and σ is the standard deviation (in natural log units) of the distribution. *Brandvik et al*. [2013a] identify σ as 0.78 for their data. They also show that dispersants can decrease interfacial tension (γ) by about 200 fold implying roughly an order of magnitude reduction in droplet size. In these simulations, the value of d_{50} = 0.069 cm was used when dispersants were applied; d_{50} = 1.03 cm was used in simulations without dispersant application (Table 1 and Figure 1). These volume distributions are associated with 73%, 37%, and 0.13% of the oil volume included in droplets > 9 mm in diameter for the "No Dispersant," "50% Efficiency" and "100% Efficiency" cases, respectively. Similar predictions have been made using the VDROP-J model [*Zhao et al*., 2014], which indicate that 50% and ~0% of the oil volume was found in > 9 mm droplets at 10 m above the cut riser under conditions without dispersants and with dispersants, respectively.

The droplet diameter distributions predicted from *Johansen et al*. [2013] and *Brandvik et al*. [2013b] included droplets with large diameters (> 2 cm). According to *Clift et al*. [1978], there is a maximum stable droplet size associated with the interfacial tension of oil. Given an interfacial tension of 23 $g\ s^{-2}$ without dispersant and 0.11 $g\ s^{-2}$ with dispersant treatment, the maximum stable droplet diameter would be 14.4 mm and 1.0 mm for each treatment respectively. Because these values were less than the maximal values predicted

from the distributions in this study (Figure 1), the volume associated with all oil droplets greater than the maximal stable values was aggregated into the highest stable value, effectively truncating the distributions in Figure 1 to the maximum stable droplet diameter.

2.1.2. Height Above Bottom

In order to estimate the height above bottom for the initial conditions for LTRANS, phase separation of gas and oil as well as oil droplet behavior needed to be parameterized. Droplets and bubbles in a multiphase plume tend to separate from the entrained seawater due to 1) ambient crossflow and/or 2) ambient stratification. The relative importance of these two processes is governed by the magnitudes of the ambient current speed U_a, and the slip velocity U_s, in relationship to the characteristic plume velocity $U_c = (B_o N)^{1/4}$ where B_o is the kinematic buoyancy flux of the oil/gas mixture, and N is the ambient stratification frequency. For a gas and oil plume, the gas bubble slip velocity should be used. *Socolofsky and Adams* [2002] characterized a plume as crossflow dominated if the ambient current causes the dispersed phases to separate from the plume before ambient stratification causes trapping. *Socolofsky et al*. [2011] used a similar criterion but substituted the plume peeling height for the trap height which predicted crossflow dominance at a somewhat smaller current speed. In general, these two assumptions lead to an approximate expression for the critical current speed $U_{a,crit}$ given by:

$$\left(U_{a,crit}/U_c\right) = a(U_c/U_s)^2 \tag{8}$$

where the coefficient a is approximately one using the peel height criterion and two using the trap height criterion. Thus for $U_a > U_{a,crit}$, conditions are crossflow dominated while for $U_a < U_{a,crit}$ they are stratification dominated. Considering conditions after the riser was cut and using representative values of $B_o = 0.49$ to 0.98 $m^4\ s^{-3}$ and $N = 0.001\ s^{-1}$ [*Socolofsky et al*., 2011], leads to $U_c = 15$-18 cm s^{-1}. Using a gas bubble slip velocity of 21 cm s^{-1} [*Socolofsky et al*., 2011], and considering a range of a = 1-2, $U_{a,crit}$ from equation (8) ranges between 8-26 cm s^{-1}. As observed currents were generally less than this range (0.5 to 10 cm s^{-1}), the plume would be classified as stratification dominated [*Socolofsky et al*., 2011]. For a stratification-dominated plume, the trap height (h_t) of the intrusion (i.e., the height above bottom) is given by *Socolofsky and Adams* [2005] and *Socolofsky et al*. [2011] as

$$h_t/\left(B_o/N^3\right)^{1/4} = 2.9\exp\left(-\left(U_s/(B_o N)^{1/4} - 1\right)^2/27\right) \tag{12}$$

while the thickness of the intrusion is given by *Akar and Jirka* [1995] as

$$h_i = 2.4U_a/N \tag{13}$$

Thus droplets are estimated to exit the intrusion at an elevation above the release point of $h_t + h_i/2$.

2.1.3. Horizontal Spread of Droplets

The horizontal spread of droplets at the trap height was estimated based on semiempirical equations from laboratory studies. *Chan et al*. [2015] studied the behavior of small glass beads released continuously at the top of a quiescent stratified tank simulating, in an inverted manner, oil droplets released continuously at the bottom of a stratified ocean. They found that if the beads/droplets were small enough (hence their slip velocity U_s was low enough), the beads would follow the entrained seawater into the intrusion, and they arrived at a critical value of $U_N = U_s/U_c = 0.3$. That is, for $U_N < 0.3$, droplets would intrude. It was found that that the radial intrusion flow rate for a multiphase plume in stratification [*Socolofsky and Adams*, 2003, 2005] was

$$Q_i = \left[0.9 - 0.38(U_s/U_c)^{0.24}\right] B^{3/8}/N^{5/8} \tag{9}$$

which allows one to compute the transport of oil droplets within the intrusion. Because droplets are expected to be vertically well-mixed within an intrusion, their rise out of the intrusion can be treated as a first order process with rate constant U_s/h_i where h_i is the intrusion thickness. The distribution of radial exit locations, C(r) is Gaussian,

$$C(r) = C_{max} e^{\frac{-r^2}{\sigma_r^2}} \tag{10}$$

where the standard deviation is given by

$$\sigma_r = ([0.9-0.39(U_s/U_c)^{0.24}]/\pi U_s)^{1/2} B^{3/8}/N^{5/8} \quad (11)$$

σ_r can also be shown to be the radial distance that a single droplet would be "broadcast" if it were to rise by plug flow from the bottom of the intrusion [*Chan et al*., 2015]. If there are multiple droplet sizes within a plume, *Chan et al*. [2015] found that droplets behave independently of droplets of other sizes as long as the plume buoyancy B is based on the total buoyancy of all contributing droplets/bubbles. Also, while equation (11) was derived for $U_N < 0.3$, *Chan et al*. [2015] found that it could be extrapolated satisfactorily to values of U_N as large as 1.4. In this study, fixed values of buoyancy flux B and stratification N ($B = 0.49\ m^4\ s^{-3}$, $N = 0.0012\ s^{-1}$) were used to compute σ_r.

In this framework as described, the distributions of droplets of different sizes would overlap. For example, a large diameter droplet with high slip velocity would have a small value of σ_r, but the random number approach for distributing droplets could put this particular particle as far as $2*\sigma_r$ from the source. Meanwhile, a small droplet with low slip velocity and large σ_r, that was placed randomly at a distance of $0.1*\sigma_r$ from the source, might actually be closer to the source than the large droplet, allowing for overlap in the spatial distributions of the droplets. In view of the overlap, it would be tempting to amass a single distribution of radial starting positions based on the two contributing distributions, but at each radial distance there would be particles of different size, and hence different slip velocities that would govern their ascent in LTRANS, after they left the intrusions. Thus, we developed a number of radial distances for each of a number of slip velocities.

As an example, assume the plume was being treated with subsurface dispersants resulting in a value of $d_{50} = 0.069$ cm (Table 1). The distribution of droplet sizes surrounding d_{50} is given by equation (7), where it is assumed that the laboratory value of $\sigma = 0.78$ holds for oceanographic conditions as well. Because smaller droplets spend longer periods within the intrusion, they were estimated to be more widely distributed horizontally when they eventually exit the intrusion. To model this behavior, the 2-dimensional distribution of droplets exiting the intrusion was computed based on their rise velocity $U_{s,i}$ (calculated according to *Zheng and Yapa* [2000]) and their resulting standard deviation $\sigma_{r,i}$ calculated with equation (11). A random number generator (Mersenne Twister, http://www.math.sci.hiroshima-u.ac.jp/~m-mat/MT/emt.html) was used to distribute particles of each size in circular coordinates (r and z), where r is the horizontal distance from the release point (and thus the peak concentration exists at $r = 0$ and a standard deviation of $\sigma_{r,i}$) and z is depth ($z = h_t + h_i/2$). For mild currents, which were observed around the time of the riser cut ($1.6\ cm\ s^{-1}$), a uniform azimuthal distribution would be reasonable, which we assumed. Note that for stronger currents, including those generated by topographic Rossby waves, the distribution would likely be skewed toward the downstream direction [*Hamilton*, 2009; *Oey and Lee*, 2002]. Note that under these conditions, the vertical location of all droplets would be the same at a given time. However, significant variation in droplet elevation was expected over time since a number of factors are strongly time-varying. For example the gas-oil ratio, and hence the void fraction n, appears to vary on a time scale of minutes [*FRTG*, 2010, p 67] while subsurface dispersants were turned on and off at least once a day [*Lehr et al*., 2010]. Too few data existed to resolve this time-variability.

In summary, the semiempirical equations above were used to determine the number and size of droplets for each dispersant case, as well as their location (depth and horizontal distance from cut riser), all of which were used as input for the far-field Lagrangian transport model.

2.2. Far-Field Model

Oil droplet transport in the far-field was simulated with LTRANS which was forced with the 3-D hydrodynamic predictions of SABGOM.

2.2.1. SABGOM

The SABGOM circulation hindcast model was implemented based on the Regional Ocean Modeling System (ROMS) [*Haidvogel et al*., 2000, 2008; *Shchepetkin and McWilliams*, 2005]. The model domain encompasses the entire South Atlantic Bight and Gulf of Mexico [*Hyun and He*, 2010; *Xue et al*., 2015, 2013]. Its spatial resolution was 5 km and included 36 vertical layers which were weighted to better resolve surface and bottom boundary layers. For both momentum and buoyancy forcing at the model surface, 3 hourly, 32 km horizontal resolution North American Regional Reanalysis (NARR, www.cdc.noaa.gov) was utilized. For open boundary conditions, SABGOM ROMS was one-way nested inside the 1/12° data assimilative North Atlantic Hybrid Coordinate Ocean Model (DA HYCOM) [*Chassignet et al*., 2009]. Refined local dynamics including 8 realistic

tidal constituents and runoff of major rivers in the region were included in SABGOM. During the DWH event, SABGOM was run in the forecast mode to provide flow fields for multiple-model surface oil trajectory forecasts [*Liu et al*., 2011; *MacFadyen et al*., 2011]. For this study, SABGOM was run in a continuous hindcast mode to provide input to the Lagrangian oil droplet model (described below). A weak relaxation scheme was imposed during the hindcast to relax SABGOM simulated temperature and salinity back to HYCOM/NCODA water mass fields over a 30-day time scale. This procedure allowed SABGOM to evolve continuously according to its own high resolution dynamics, and at the same time be on par with data assimilative HYCOM model prediction at the low frequency. Extensive model-data validations have shown that SABGOM provided a realistic circulation hindcast for this study. Simulation output was stored hourly to resolve changes in current velocities at tidal time scales and included three-dimensional fields of temperature, salinity, density, and diffusivities, three components of velocity, and sea surface height for use in LTRANS.

2.2.2. LTRANS

LTRANS [*North et al*., 2008, 2011, 2015; *Schlag and North*, 2012] was used to predict oil droplet transport using the stored predictions of SABGOM. LTRANS is an open source off-line particle-tracking model (http://northweb.hpl.umces.edu/LTRANS.htm) that tracks the trajectories of particles (or droplets) in three dimensions using advection, stochastic diffusion, and behavior such as oil droplet rise velocities [*North et al*., 2011, 2015]. LTRANS used predictions from SABGOM to calculate the movement of droplets in 5-min intervals by interpolating sea surface height, three components of velocities, salinity, temperature, and vertical diffusivity from the SABGOM grid to the droplet location. Dynamic viscosity was determined after interpolating SABGOM salinity and temperature to the droplet location. LTRANS included a 4th order Runge-Kutta scheme for droplet advection and a random displacement model for vertical subgrid scale turbulent diffusion [*Visser*, 1997]. For horizontal subgrid scale turbulent diffusion, a random walk model was applied using a constant horizontal diffusivity of 1 $m^2\ s^{-1}$. Oil droplet rise velocities were based on equations in *Zheng and Yapa* [2000] and oil droplet density was fixed at 858 kg m^{-3} (reported in *Lehr et al*. [2010] and used by *Socolofsky et al*. [2011]). Vertical boundary conditions were reflective if a droplet passed through the surface or bottom boundary due to turbulence or vertical advection. If a droplet passed through the surface due to oil droplet rise velocity, then the droplet was placed just below the surface (i.e., it stopped near the boundary).

2.2.3. Model Experiments

A series of experiments were conducted using LTRANS to explore the competing effects of hydrodynamic forcing and dispersant application on the timing, mass and spatial extent of oil as it reached the surface. The three dispersant scenarios (no dispersants, dispersant application with 50% efficiency, and dispersant application with 100% efficiency) were repeated under five different hydrodynamic regimes for a total of 15 simulations. The hydrodynamic regimes included (1) no advection, diffusion, or turbulence, (2) vertical turbulence only, (3) horizontal turbulence only, (4) 3-D advection only (i.e., 3-D current velocities), and (5) a full realization of vertical and horizontal turbulence combined with 3-D current velocities from the SABGOM model. While the mass of oil that was released in each simulation was constant across model runs, the diameter and number of droplets differed between the no dispersant and dispersant cases (Figure 1). The simulated droplets from the near-field model were released into the far field model every five minutes for 3 h, beginning at 2 AM on 3 June 2010 with an oil flow rate of 60,800 bbl d^{-1} [*McNutt et al*., 2012], which was between the typical flow rates observed before and after the riser cut. Given the volume of oil released, it was unrealistic to simulate every oil droplet that may have been present. Instead, a subset of oil droplets was simulated to represent the entire volume (Simulated Oil Volume = Total Oil Volume/R_s, where $R_s = 10^4$ for the no-dispersant case and 10^7 for the dispersant case). Tests of the sensitivity of model predictions to increases and decreases in the number of simulated droplets were conducted by varying R_s by a factor of 10^3. Minimal effects were found so the runs were conducted with 1,205,820 and 7,978,896 simulated droplets for the no dispersant and dispersant cases, respectively. For each model run, droplets were tracked for 36 h after the start of the simulation. Predictions were analyzed to examine the potential influence of hydrodynamics and dispersant application on the timing, mass and spatial extent of oil as it reached the surface.

To isolate the effects of subsurface dispersant application on droplet sizes and the subsequent change in surface expression of oil, the effects of dissolution and biodegradation were not included in the model. Thus results provide information on the sensitivity of model predictions to hydrodynamics and droplet size alone and neglect potential changes in density and diameter over time as the droplets moved within the model. It is likely that the assumption of no biodegradation was reasonable because bacterial colonization of oil droplets is on the order of days [*Lee et al*., 2013; *MacNaughton et al*., 2003] and the duration of these numerical experiments was

limited to 36 h. The assumption of no dissolution in these model runs likely biased the simulated droplets toward rising faster than reality because rapid dissolution of the lightest hydrocarbon compounds would have resulted in smaller denser droplets that remained in the water column for longer periods. Had dissolution been included, it likely would have had a greater effect on smaller droplets than larger droplets due to the larger surface area to volume ratio of smaller droplets. Hence, model results herein could be considered a conservative estimate of the influence of dispersants on the surface expression of oil.

3. Results

Comparison of model predictions with reports of the timing and spatial extent of surfacing oil indicated that the model simulated features of the surfacing of oil droplets that resemble those observed during the *Deepwater Horizon* spill. Simulated oil droplets began to reach the surface between 3 and 4 h after droplet release initiated in the no-dispersant and 50% efficiency dispersant simulations (Figure 2). This time interval corresponded with the ~3 h lag in changes in the surfacing slick after a deliberate intervention at the well head which was reported by observers on response vessels [*Ryerson et al*., 2012]. In addition, the diameter of the surfacing plume of simulated droplets was ~1.8 km (Figures 3e, 3j, and 3o), similar to the observed zone of surfacing mass of ~1.6 km in diameter reported by *Ryerson et al*. [2012].

The most striking effect of simulated dispersant application at the wellhead was the amount of oil which surfaced within a given time. In the no-dispersant cases, 100% of the oil mass released in the experiment reached the surface within 7 h (Figure 2), yet only 49% and 0% had reached surface in the 50% and 100% efficiency cases, respectively, in the same amount of time. After 12 h, only 61% and 28% of the oil reached the surface in the 50% and 100% dispersant efficiency cases, respectively. The 50% dispersant efficiency scenario resulted in overall weaker surface expression than the no-dispersant case, with 74% of the released oil reaching the surface after 18 h. This also contrasts with the 100% dispersant efficiency case, where only 48% of the oil released was transported to the surface after 18 h and 73% after 36 h (Figure 2).

The transport of oil droplets in all of experiments was related to their size, and thus, their interaction with dispersants. The droplets that exceeded 5 mm in diameter rose to the surface within several hours, and were transported 1-5 km horizontally via relatively rapid surface currents (10-35 cm s^{-1} at depths $<$ 10 m versus ~1.6 cm s^{-1} at depths $>$ 100 m) (Figure 3). Intermediate-sized droplets (0.2 to 2 mm in diameter) rose gradually in the water column, reaching the surface in 5–8 h after being spread out horizontally by 0.5 to 1 km during their rise, primarily by horizontal turbulence (Figure 3). Smaller droplets, including the majority of droplets treated by dispersants, were spread horizontally (Figure 3) and rose sufficiently slowly that they remained deep in the water-column after 36 h (not shown). The horizontal distribution of droplets in the subsurface was primarily driven by horizontal turbulence, because simulations with only vertical turbulence and advection resulted in far less horizontal spread of oil droplets (Figure 3). A slight westward bulge in the droplet plume at 600-800 m was associated with westward advection at these depths (Figure 3).

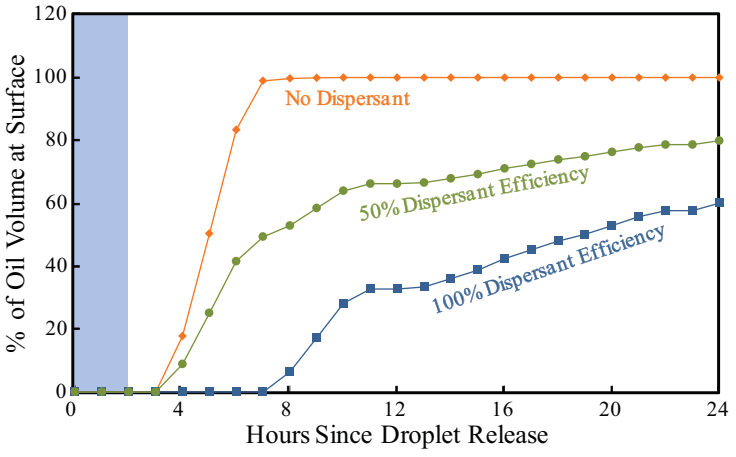

Figure 2. Percent of total oil volume that reached the surface (depth $<$ 2 m) at a given time for simulations without dispersants (orange) and with dispersants applied at the wellhead with 50% efficiency (green) and 100% efficiency (blue) scenarios. The blue shaded box indicates the time period during which oil droplets were released into the far-field model.

Upon reaching the surface, oil droplets were transported horizontally, with a slightly northwest trajectory (Figure 4). In the no-dispersant and 50% dispersant efficiency treatments, a ~2 km surface plume developed at the surface within 4-6 h, while few droplets had reached the surface at this time in the 100% dispersant efficiency case (Figure 4). The area of this surfacing plume of oil was driven by the spatial extent of the intermediately-sized

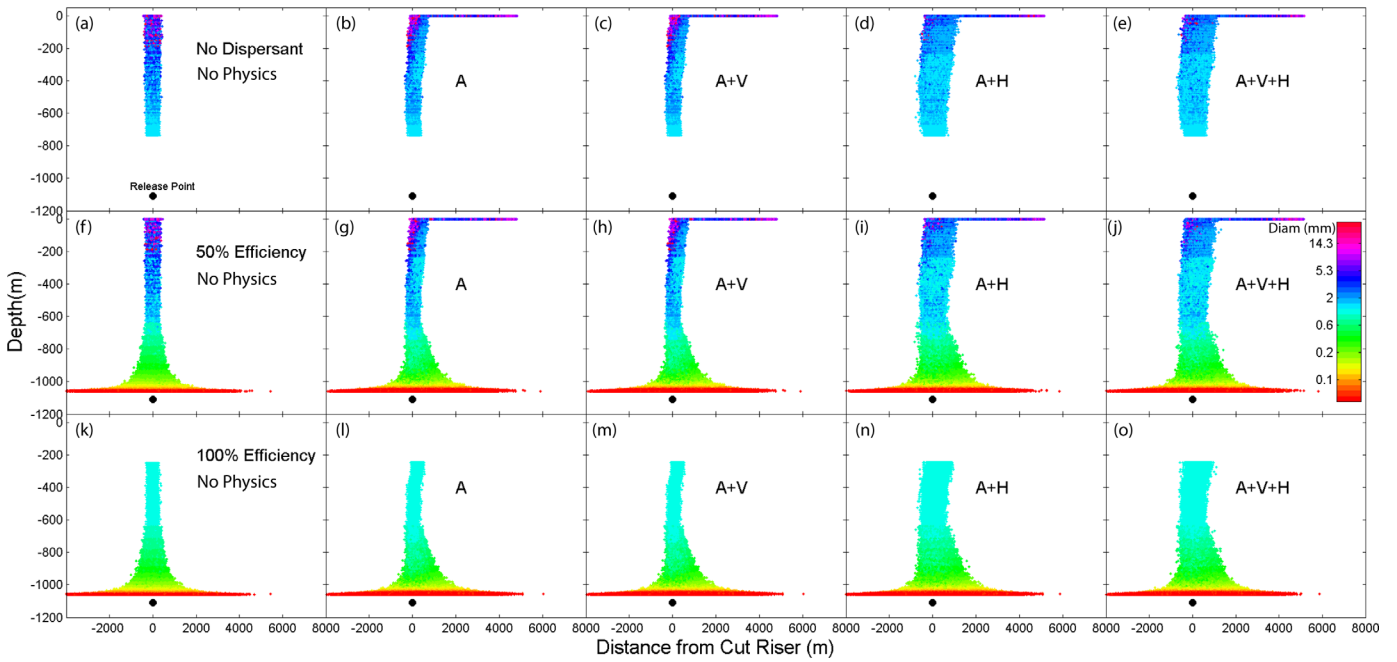

Figure 3. Vertical distribution of oil droplets 6 h after the start of model simulations (a-e) without dispersants and with dispersants applied at the wellhead with (f-j) 50% efficiency and (k-o) 100% efficiency. Colors represent droplet sizes (see legend in Figure 3j). Model predictions with varying levels of hydrodynamic forcing are shown: (a, f, k) without hydrodynamics, (b, g, l) advection (A) only, (c, h, m) advection plus vertical turbulence (V), (d, i, n) advection plus horizontal turbulence (H), and (e, j, o) advection plus vertical and horizontal turbulence.

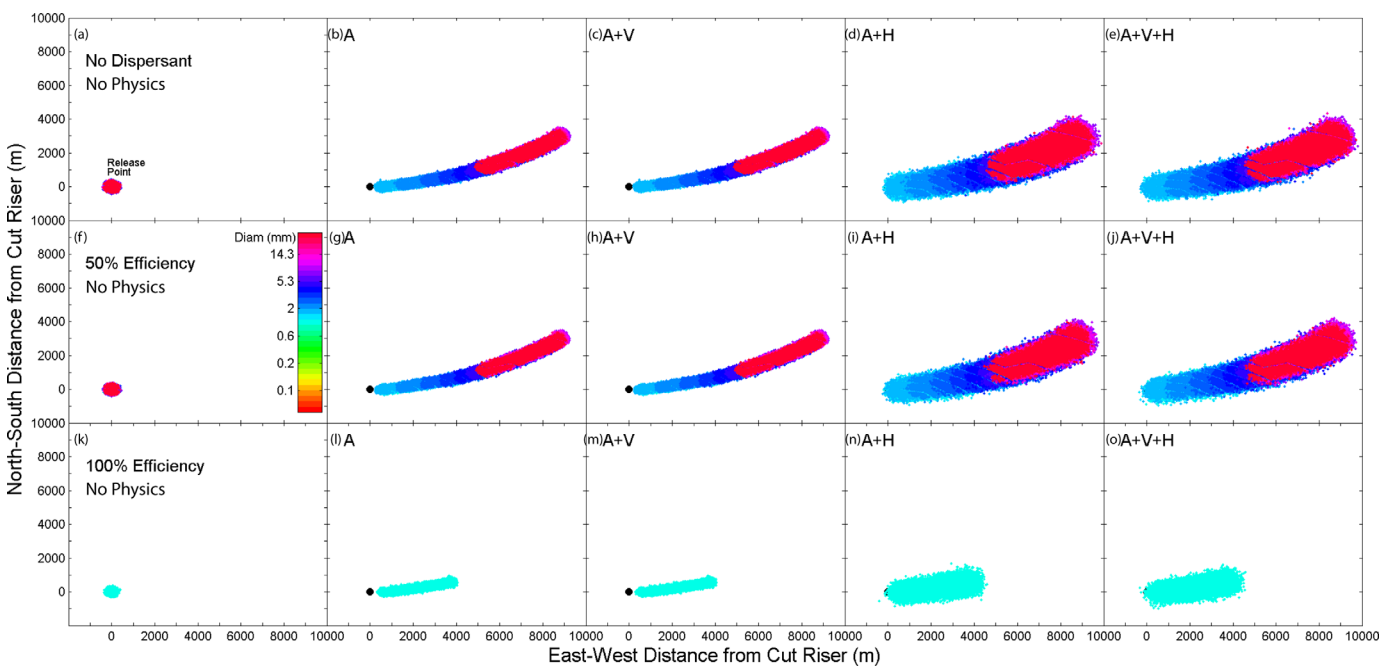

Figure 4. Map-view of the distribution of oil droplets at the water surface (depth < 2 m) 6 h after the start of model simulations (a-e) without dispersants and with dispersants applied at the wellhead with (f-j) 50% efficiency and (k-o) 100% efficiency. Colors represent droplet sizes (see legend in Figure 4f). Model predictions with varying levels of hydrodynamic forcing are shown: (a, f, k) without hydrodynamics, (b, g, l) advection (A) only, (c, h, m) advection plus vertical turbulence (V), (d,i,n) advection plus horizontal turbulence (H), and (e, j, o) advection plus vertical and horizontal turbulence.

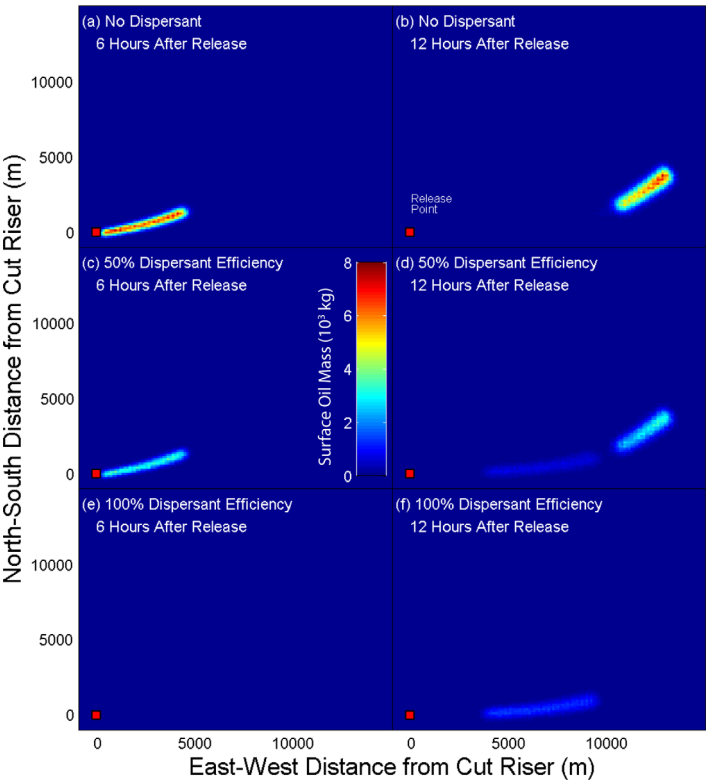

Figure 5. Distribution of total oil mass at the water surface (depth $<$ 2 m) in simulations (a-b) without dispersants and with dispersants applied at the wellhead with (c-d) 50% efficiency and (e-f) 100% efficiency. (left) Mass at the surface 6 h after the start of model simulations; (right) Mass distributions 12 h after the start. Note that droplets release into the model domain stopped after the first 3 h of each simulation which resulted in the break in the surface slick from the location of the wellhead (red square) seen in the plots on the right.

droplets (1-5 mm), because the larger, rapidly rising droplets reached the surface in a relatively narrow horizontal band that was less influenced by horizontal turbulence than the smaller droplets (Figure 3). In the absence of horizontal turbulence, the area of the surfacing oil was 50% smaller when only the forces of vertical turbulence or vertical plus horizontal advection acted on the rising oil droplets. Upon converting the number of oil droplets to total mass of oil in the surface ($<$ 2 m depth) for each scenario, it was found that the application of dispersants reduced the maximum mass of surface oil after 12 h by 75% (from 8000 kg to 2000 kg), although the spatial distributions of water that contained some amount of oil were similar (Figure 5).

4. Discussion

Model simulations indicated that the timing, mass, and spatial extent of oil as it reached the surface was highly sensitive to dispersant application under conditions similar to the *Deepwater Horizon* event. When dispersants were applied in the model, less oil reached the surface, the oil that reached the surface arrived there more slowly, and the spatial extent of the surface slick was diminished compared to the scenarios without dispersants. These findings suggest that application of dispersants at the well head of deep water blowouts could slow the surfacing of oil, that the oil could have a longer residence time in the water-column, and that the oil would be more highly influenced by subsurface transport. In a model intercomparison study, *Socolofsky et al*. [2015] also found that dispersant application at the well head could result in a significant fraction of oil remaining in the subsurface. The strong effect of dispersant application which was found in our model simulations was due to the predicted size of droplets formed in the near-field plume and on the change in the size of droplets upon application of dispersants. This research suggests that observations of droplet size distributions and a better understanding of the effect of dispersant application at well heads during deep water oil spills are important for understanding and predicting both the short-term and long-term fate and transport of oil from deep water blowouts.

Model simulations were designed to better understand the role of droplet size on the short-term fate of oil under the conditions that followed the cutting of the collapsed riser on 3 June 2010 and indicated that dispersant treatments, even if only 50% efficient, were effective in keeping $>$30% of the released oil from surfacing over the duration of the simulations (36 h). These simulation results were consistent with the estimates that at least 30% of the total oil released during the *Deepwater Horizon* spill could have been retained in deep waters [*Joye et al*., 2014; *Ryerson et al*., 2012].

Although it is unclear from an oil spill abatement perspective if subsurface retention is more desirable than surfacing, one would expect the transport trajectory of oil to be quite different in the surface relative to deeper waters [*North et al*., 2011], an idea supported by this modeling study and inferred from previous

investigations [*DeHaan and Sturges*, 2005; *Welsh and Inoue*, 2000]. Because current velocities were much lower at depth than at the surface during these simulations, the oil retained in the subsurface was not significantly transported horizontally in the 36 h following its release. A large fraction of the small-diameter oil droplets (and their associated volume) was retained between 1000 and 1200 m deep, consistent with observations [*Ryerson et al*., 2012; *Socolofsky et al*., 2011] during the *Deepwater Horizon* spill. In contrast to the rapidly rising droplets, simulations of smaller droplets indicated that small oil droplets covered a horizontal distance in excess of 12 km near the exit of the intrusion (Figure 3), which is well within the observed extent of the subsurface plume [*Camilli et al*., 2010].

A notable conclusion of this analysis was the sensitivity of model predictions to the parameterization of horizontal turbulent particle motion. Although horizontal advection during the simulations resulted in a slight net westward transport of the intermediate droplet sizes around 1000 m (Figure 3), the primary effect of advection was at the surface where oil was transported rapidly away from the area of release. Modeled vertical advection, which was bi-directional during the course of the simulations, did not exceed 0.06 cm s^{-1} and was much smaller than the computed rise velocities of $>$0.5 cm s^{-1} for most of the oil droplet size classes ($>$ 0.3 mm). In contrast, the addition of horizontal turbulence widened the horizontal extent of the rising plume by $\sim$1.5 km (relative to vertical turbulence+advection only case), which was sufficient to produce a surfacing plume of $\sim$1.8 km diameter that was consistent with observations soon after the riser was cut on 3 June [*Ryerson et al*., 2012]. The constant horizontal diffusivity used in the model was 1 m^2 s^{-1} and is within reasonable values for horizontal turbulence in a coastal system [*Csanady*, 1973] but is perhaps the least constrained parameter in Lagrangian models because it is used to simulate horizontal mixing below the grid scale of the model, not necessarily horizontal turbulence per se. Although the results of this study suggest that a constant value of 1 m^2 s^{-1} may be reasonable because of the similarity of model predictions with observations, the sensitivity of model predictions to horizontal turbulence indicates that a more systematic study of the parameterization of horizontal subgrid scale turbulence in Lagrangian models would be warranted.

Although model results advance understanding of the influence of droplet size and dispersants on oil fate and transport, it is important to note that these model simulations did not include many important processes that influence the weathering of oil, such as dissolution, biodegradation, emulsification, evaporation, wave-induced dispersion, and photodegradation. Thus, the model simulations presented here are intended to simulate only the short-term effects of dispersant-induced droplet size reductions. The degradation of oil within the Gulf of Mexico is expected to occur via different pathways in surface water versus deeper water. In deep, subsurface waters, microbial degradation of hydrocarbons should be the dominant loss term for oil, and although microbial degradation has been documented [*Hazen et al*., 2010; *Valentine et al*., 2010], it is unclear how much of the total hydrocarbon release associated with *Deepwater Horizon* was degraded in the subsurface. Experimental studies have revealed that the nongaseous, straight-chain components of the hydrocarbon pool degrade at rates of 0.5 μM C d^{-1}, which is relatively slow given the potential for an associated residence time of these compounds in the deep Gulf of Mexico to be multiple months or longer [*Camilli et al*., 2010]. At the surface, oil will be degraded by photolysis and reduced via volatization [*Haritash and Kaushik*, 2009], while the breaking of surface waves will reduce oil droplet size and consequently, increase its degradation rate. Microbial communities in surface waters are also different from those of colder, deeper waters, which may affect the rate of hydrocarbon degradation [*Redmond and Valentine*, 2012]. Considering the time-scales of the above processes (minutes-days), the microbial degradation terms should start affecting the droplet dynamics after 1-2 days, which is why these analyses were focused on rising oil droplets and the hours immediately following their release from the cut riser. In addition to microbial degradation and dissolution, the surface processes stated above (e.g., waves), as well as the effects of evaporation and water-oil emulsions, have the potential to alter the size and distribution of surface slicks over periods greater than simulated here [*Zeinstra-Helfrich et al*., 2015]. Many oil spill response models include these processes to allow for more realistic long-term simulations; these processes would be important to include in future sensitivity studies with the model herein.

Previous modeling studies of oil transport in the Gulf of Mexico following the initiation of the *Deepwater Horizon* oil spill have revealed a number of important insights into both near- and far-field transport of oil in response to environmental conditions. The results of this study indicated rapid surface expression of oil in the absence of dispersant (Figure 3), owing to the relatively large oil droplets simulated (73% of

volume > 9 mm diameter). Recent studies have simulated a smaller volume fraction of these larger oil droplets [*North et al*., 2015; *Socolofsky et al*., 2015; *Zhao et al*., 2014]. The droplet sizes in the 50% efficiency simulations were consistent with these other studies. Simulations with larger droplet sizes, as in the "No Dispersant" case, included faster ascent times and, in the context of the simulations presented here, resulted in a ~20% increase in the volume of oil reaching the surface over a 24 h period. *North et al*. [2015] illustrated that oil droplets with diameters 0.3 mm and greater, which were some of the smaller droplets in this study, were efficiently moved to the surface despite varying rates of potential biodegradation. Thus it is possible that a large fraction (~50-70% in our simulations) of the oil could have reached the surface, even when dispersants were applied (assuming 50% efficiency). Ultimately, characteristics of this oil once it reaches the surface (e.g., thickness, visibility as a sheen), which we did not model explicitly, determine its ultimate recoverability or treatment.

It was assumed that the volume of any predicted oil droplet from the log-normal distribution of diameters which exceeded the maximum droplet size under the given conditions [*Clift et al*., 1978] would have the diameter of the largest stable droplet size upon breakup. Consequently, large volumes were simulated for the largest stable droplet size class (Figure 1). It is possible that this approach is not realistic, but given that the unstable droplets might follow many different pathways to reaching stable sizes (e.g., split in half versus split into many droplets; split up once versus multiple splits), it is unclear how this droplet size reduction should be modeled. We consider our approach to be the most conservative formulation that minimizes differences between simulations, but recognize that alternative formulations are certainly possible. Future experimental research on unstable droplet behavior would provide the insights necessary to improve our approach.

The current study provides an example of the utility of LTRANS (and particle tracking models in general) for tracking the fate and transport of oil released during accidental oil injections into the environment. These results emphasize how the coupling of empirical formulations of oil behavior with physical transport and particle tracking models can inform the understanding of how dispersants affect the fate of oil in natural waters. Although many types of models have been applied to realistically simulate the dynamics of oil spills (GNOME [*Zelenke et al*., 2012], CDOG [*Zheng et al*., 2003], OILTRANS [*Berry et al*., 2012], BLOSOM [*Paris et al*., 2012], OILMAP [*Spaulding et al*., 1994], SIMAP [*French McCay*, 2003], OSCAR [*Reed et al*., 1995], and many more), here we focused on a suite of sensitivity tests that target conditions similar to the Deepwater Horizon event using a model package that is of intermediate complexity relative to two-dimensional surface slick models and three-dimensional oil spill fate and transport models. The simulations presented here display the short-term (1-2 days) behavior of oil droplets, yet projections further into the future are possible given enhancements to the behavior and natural reactions of oil to represent additional processes. Additional processes to be built into LTRANS include the dissolution of oil following its release, the effects of surface waves and photodegradation on oil once it reaches surface waters, and the interaction of oil with other materials (e.g., suspended particles) in the water-column and sediments [*Passow et al*., 2012; *Reddy et al*., 2012].

Acknowledgments

We would like to thank Ian Mitchell for support and assistance with LTRANS simulations and two anonymous reviewers for their comments which improved the manuscript. Funding for this project was supported by the BP/Gulf of Mexico Research Initiative through the Gulf Integrated Spill Response (GISR) consortium. In addition, EA received support from the API Joint Industry Task Force D3 Subsurface Dispersant Injection team. The model output included in this analysis will be made available upon written request to the corresponding author, Jeremy Testa (jtesta@umces.edu) and the code is publicly available through the Gulf of Mexico Research Initiative Information & Data Cooperative (GRIIDC) at https://data.gulfresearchinitiative.org (doi:10.7266/N7RX9931). This is contribution number 5210 of the University of Maryland Center for Environmental Science.

References

Akar, P. J., and G. H. Jirka (1995), Buoyant spreading processes in pollutant transport and mixing Part 2: Upstream spreading in weak ambient current, *J. Hydraul. Res.*, *33*, 87–100.

Berry, A., T. Dabraowski, and K. Lyons (2012), The oil spill model OILTRANS and its application to the Celtic Sea, *Mar. Pollut. Bull.*, *64*, 2489–2501.

Brandvik, P. J., Ø. Johansen, F. Leirvik, U. Farooq, and P. S. Daling (2013a), Droplet breakup in subsurface oil releases-Part 1: Experimental study of droplet breakup and effectiveness of dispersant injection, *Mar. Pollut. Bull.*, *73*(1), 319–326.

Brandvik, P. J., O. Johansen, U. Farooq, G. Angell, and F. Leirvik (2013b), *Sub-Surface Oil Releases-Experimental Study of Droplet Distributions and Different Dispersant Injection Techniques. A Scaled Experimental Approach Using the SINTEF Tower Basin*, SINTEF Materials and Chemistry, Trondheim, Norway.

Camilli, R., C. M. Reddy, D. R. Yoerger, B. A. S. V. Mooy, M. V. Jakuba, J. C. Kinsey, C. P. McIntyre, S. P. Sylva, and J. V. Maloney (2010), Tracking hydrocarbon plume transport and biodegradation at Deepwater Horizon, *Science*, *330*(6001), 201–204.

Chan, G. K. Y., A.C. Chow, and E. E. Adams (2015), Effects of droplet size on intrusion of sub-surface oil spills, *Environ. Fluid Mech.*, *15*(5), 959–973.

Chang, Y.-L., L. Oey, F.-H. Xu, H.-F.Lu, and A. Fujisaki (2011), 2010 Oil Spill - trajectory projections based on ensemble drifter analyses, *Ocean Dyn.*, *61*, 829–839, doi:10.1007/s10236-10011-10397-10234.

Chassignet, E. P., et al. (2009), U.S. GODAE: Global Ocean Prediction with the HYbrid Coordinate Ocean Model (HYCOM), *Oceanography*, *22*(2), 64–75.

Clift, R., J. R. Grace, and M. E. Weber (1978), *Bubbles, Drops, and Particles*, Academic, N. Y.

Csanady, G. T. (1973), *Turbulent Diffusion in the Environment*, D. Reidel, Dordrecht, Netherlands.
DeHaan, C. J., and W. Sturges (2005), Deep cyclonic circulation in the Gulf of Mexico, *J. Phys. Oceanogr.*, *35*, 1801–1812.
Dehkharghanian, V., and S. A. Socolofsky (2014), Comparing different dispersant injection mechanisms into subsea oil-well blowout using PLIF method, paper presented at 7th International Symposium on Environmental Hydraulics, International Association of Hydro-Environment Engineering and Research (IAHR), Singapore.
French McCay, D. P. (2003), Development and application of damage assessment modeling: Example assessment for the North Cape Oil Spill, *Mar. Pollut. Bull.*, *477*, 341–359.
FRTG (2010), *Deepwater Horizon Release Estimate of Rate by PIV*, U.S. Geol. Surv., Washington, D. C. [Avaialble at https://www.doi.gov/sites/doi.gov/files/migrated/deepwaterhorizon/upload/FRTG-report-Appendix-D-Plume-Analysis-Report.pdf.]
Haidvogel, D. B., H. G. Arango, K. Hedstrom, A. Beckmann, P. Malanotte-Rizzoli, and A. F. Shchepetkin (2000), Model evaluation experiments in the North Atlantic Basin: Simulations in nonlinear terrain-following coordinates, *Dyn. Atmos. Oceans*, *32*(3), 239–281.
Haidvogel, D. B., et al. (2008), Ocean forecasting in terrain-following coordinates: Formulation and skill assessment of the Regional Ocean Modeling System, *J. Comput. Phys.*, *227*, 3595–3624.
Hamilton, P. (2009), Topographic Rossby waves in the Gulf of Mexico, *Prog. Oceanogr. 82*(1), 1–31.
Haritash, A. K., and C. P. Kaushik (2009), Biodegradation aspects of polycyclic aromatic hydrocarbons (PAHs): A review, *J. Hazard. Mater. 169*(1), 1–15.
Hazen, T. C., et al. (2010), Deep-sea oil plume enriches indigenous oil-degrading bacteria, *Science*, *330*(6001), 204–208.
Hyun, K. H., and R. He (2010), Coastal upwelling in the South Atlantic Bight: A revisit of the 2003 cold event using long term observations and model hindcast solutions, *J. Mar. Syst.*, *83*, 1–13.
Johansen, O., P. J. Brandvik, and U. Farooq (2013), Droplet breakup in subsea oil releases–-Part 2: Prediction of droplet size distributions with and without injection of chemical dispersants, *Mar. Pollut. Bull.*, *73*, 327–335.
Joye, S. B., A.P. Teske, and J.E. Kostka (2014), Microbial dynamics following the macondo oil well blowout across Gulf of Mexico environments, *BioScience*, *64*(9), 766–777.
Kujawinski, E. B., M. C. Kido Soule, D. L. Valentine, A. K. Boysen, K. Longnecker, and M. C. Redmond (2011), Fate of dispersants associated with the Deepwater Horizon oil spill, *Environ. Sci. Technol.*, *45*(4), 1298–1306.
Lee, K., T. Nedwed, R. C. Prince, and D. Palandroc (2013), Lab tests on the biodegradation of chemically dispersed oil should consider the rapid dilution that occurs at sea, *Mar. Pollut. Bull.*, *73*(1), 314–318.
Lehr, B., S. Bristol, and A. Possolo (2010), Oil budget calculator-deepwater horizon, report, Fed. Interagency Solutions Group, Oil Budget Calculator Sci. and Eng. Team. [Available at http://www.restorethegulf.gov/sites/default/files/documents/pdf/OilBudgetCalc_Full_HQ-Print_111110.pdf, last accessed 27 October 2015.]
Lindo-Atichati, D., D. Lindo-Atichati, C. Paris, M. L. Hénaff, M. Schedler, A. G. Valladares-Juárez, and R. Müller (2014), Simulating the effects of droplet size, high pressure biodegradation, and variable flow rate on the subsea evolution of deep plumes from the Macondo blowout, *Deep Sea Res., Part II*, *129*, 301–310.
Liu, Y., R. H. Weisberg, C. Hu, and L. Zheng (2011), Trajectory forecast as a rapid response to the Deepwater Horizon oil spill, in *Monitoring and Modeling the Deepwater Horizon Oil Spill: A Record-Breaking Enterprise*, edited by Y. Liu, A. Macfadyen, Z. G. Ji, and R. H. Weisberg, AGU, Washington, D. C., doi:10.1029/2011GM001121.
MacFadyen, A., G. Y. Watabayashi, C. H. Barker, and C. J. Beegle-Krause (2011), Tactical modeling of surface oil transport during the Deepwater Horizon spill response, in *Monitoring and Modeling the Deepwater Horizon Oil Spill: A Record-Breaking Enterprise*, edited by Y. Liu et al., AGU, Washington, D. C., doi:10.1029/2011GM001128.
MacNaughton, S. J., R. Swannell, F. Daniel, and L. Bristow (2003), Biodegradation of dispersed Forties crude and Alaskan North Slope oils in microcosms under simulated marine conditions, *Spill Sci. Technol. Bull.*, *8*(2), 179–186.
Mariano, A. J., G. R. Halliwell, V. Kourafalou, E. Ryan, A. Srinivasan, and M. Roffer (2011), On the modeling of the 2010 Gulf of Mexico oil spill, *Dyn. Atmos. Oceans*, *52*, 322–340, doi:10.1016/j.dynatmoce.2011.1006.1001.
McNutt, M. K., R. Camilli, T. J. Crone, G. D. Guthrie, P. A. Hsieh, T. B. Ryerson, O. Savas, and F. Shaffer (2012), Review of flow rate estimates of the Deepwater Horizon oil spill, *Proc. Natl. Acad. Sci. U. S. A.*, *109*, 20,260–20,267.
North, E. W., Z. Schlag, R. R. Hood, M. Li, L. Zhong, T. Gross, and V. S. Kennedy (2008), Vertical swimming behavior influences the dispersal of simulated oyster larvae in a coupled particle-tracking and hydrodynamic model of Chesapeake Bay, *Mar. Ecol. Prog. Ser.*, *359*, 99–115.
North, E. W., E. E. Adams, Z. Schlag, C. R. Sherwood, R. He, K. H. Hyun, and S. A. Socolofsky (2011), Simulating oil droplet dispersal from the Deepwater Horizon spill with a Lagrangian approach, in *Monitoring and Modeling the Deepwater Horizon Oil Spill: A Record-Breaking Enterprise*, edited by Y. Liu et al., pp. 217–226, AGU, Washington, D. C., doi:10.1029/2011GM001102.
North, E. W., E. E. Adams, A. E. Thessen, Z. Schlag, R. He, S. A. Socolofsky, S. M. Masutani, and S. D. Peckham (2015), Assessing the influence of droplet size and biodegradation on the transport of subsurface oil droplets during the Deepwater Horizon spill: A model sensitivity study, *Environ. Res. Lett.*, *10*, 024016. [Available at http://iopscience.iop.org/021748-029326/024010/024012/024016/.]
NRC (2003), *Oil in the Sea III: Inputs, Fates, and Effects*, Natl. Acad. Press, Washington, D. C. [Available at http://www.nap.edu/catalog/10388/oil-in-the-sea-iii-inputs-fates-and-effects.]
Oey, L.-Y., and H.-C. Lee (2002), Deep eddy energy and topographic Rossby waves in the Gulf of Mexico, *J. Phys. Oceanogr.*, *32*, 3499- 3527.
Paris, C. B., M. L. Hénaff, Z. M. Aman, A. Subramaniam, J. Helgers, D.-P. Wang, V. H. Kourafalou, and A. Srinivasan (2012), Evolution of the Macondo well blowout: Simulating the effects of the circulation and synthetic dispersants on the subsea oil transport, *Environ. Sci. Technol.*, *46*(24), 13,293–13,302.
Passow, U., K. Ziervogel, V. Asper, and A. Diercks (2012), Marine snow formation in the aftermath of the Deepwater Horizon oil spill in the Gulf of Mexico, *Environ. Res. Lett.*, *7*(3).
Place, B., B. Anderson, A. Mekebri, E. T. Furlong, J. L. Gray, R. Tjeerdema, and J. Field (2010), A role for analytical chemistry in advancing our understanding of the occurrence, fate, and effects of Corexit oil dispersants, *Environ. Sci. Technol.*, *44*(16), 6016–6601.
Reddy, C. M., et al. (2012), Composition and fate of gas and oil released to the water column during the Deepwater Horizon oil spill, *Proc. Natl. Acad. Sci. U. S. A.*, *109*(50), 20,229–20,234.
Redmond, M. C., and D. L. Valentine (2012), Natural gas and temperature structured a microbial community response to the Deepwater Horizon oil spill, *Proc. Natl. Acad. Sci. U. S. A>*, *109*(50), 20,292–20,297.
Reed, M., O. M. Aamo, and P. S. Daling (1995), Quantitative analysis of alternate oil spill response strategies using OSCAR, *Spill Sci. Technol. Bull.*, *2*(1), 67–74.
Ryerson, T. B., K. C. Aikin, W. M. Angevine, E. L. Atlas, D. R. Blake, C. A. Brock, F. C. Fehsenfeld, R. S. Gao, J. A. de Gouw, and D. W. Fahey (2011), Atmospheric emissions from the Deepwater Horizon spill constrain air-water partitioning, hydrocarbon fate, and leak rate, *Geophys. Res. Lett.*, *38*, L07803, doi:10.1029/2011GL046726.

Ryerson, T. B., et al. (2012), Chemical data quantify Deepwater Horizon hydrocarbon flow rate and environmental distribution, *Proc. Natl. Acad. Sci. U. S. A.*, *109*, 20246–20253.
Schlag, Z. R., and E. W. North. (2012), Lagrangian TRANSport model (LTRANS v.2) User's Guide, 183 pp., Univ. of Md Cent. for Environ. Sci., Horn Point Lab., Cambridge.
Shchepetkin, A. F., and J. C. McWilliams (2005), The Regional Oceanic Modeling System: A split-explicit, free-surface, topography-following-coordinate oceanic model, *Ocean Modell.*, *9*, 347–404.
Socolofsky, S. A., and E. E. Adams (2002), Multi-phase plumes in uniform and stratified crossflow, *J. Hydraul. Res.*, *40*(6), 661–672.
Socolofsky, S. A., and E. E. Adams (2003), Liquid volume fluxes in stratified multiphase plumes, *J. Hydraul. Eng.*, *129*(11), 905–914.
Socolofsky, S. A., and E. E. Adams (2005), Role of slip velocity in the behavior of stratified multiphase plumes, *J. Hydraul. Eng.*, *131*(4), 273–282.
Socolofsky, S. A., E. E. Adams, and C. R. Sherwood (2011), Formation dynamics of subsurface hydrocarbon intrusions following the Deepwater Horizon blowout, *Geophys. Res. Lett.*, *38*, L09602, doi:10.1029/2011GL047174.
Socolofsky, S. A., et al. (2015), Intercomparison of oil spill prediction models for accidental blowout scenarios with and without subsea chemical dispersant injection, *Mar. Pollut. Bull.*, *96*, 110–126.
Spaulding, M. L., V. S. Kolluru, E. Anderson, and E. Howlett (1994), Application of three-dimensional oil spill model (WOSM/OILMAP) to Hindcast the Braer spill, *Spill Sci. Technol. Bull.*, *1*(1), 23–35.
Valentine, D. L., et al. (2010), Propane respiration jump-starts microbial response to a deep oil spill, *Science*, *330*(6001), 208–211.
Visser, A. W. (1997), Using random walk models to simulate the vertical distribution of particles in a turbulent water column, *Mar. Ecol. Prog. Ser.*, *158*, 275–281.
Weisberg, R. H., L. Zheng, and Y. Liu (2011), Tracking subsurface oil in the aftermath of the Deepwater Horizon well blowout, in *Monitoring and Modeling the Deepwater Horizon Oil Spill: A Record-Breaking Enterprise*, edited by Y. Liu et al., pp. 205–215, AGU, Washington, D. C., doi:10.1029/2011GM001131.
Welsh, S. E., and M. Inoue (2000), Loop current rings and the deep circulation in the Gulf of Mexico, *J. Geophys. Res.*, *107*, 16,951–16,959.
Xue, Z., R. He, K. Fennel, W. J. Cai, S. Lohrenz, and C. Hopkinson (2013), Modeling ocean circulation and biogeochemical variability in the Gulf of Mexico, *Biogeosciences*, *10*, 7219–7234.
Xue, Z., J. Zambon, Z. Yao, Y. Liu, and R. He (2015), An integrated ocean circulation, wave, atmosphere, and marine ecosystem prediction system for the South Atlantic Bight and Gulf of Mexico, *J. Oper. Oceanogr.*, *8*(1), 80–91.
Yapa, P. D., M. R. Wimalaratne, A. L. Dissanayake, and J. J.A. DeGraff (2012), How does oil and gas behave when released in deepwater?, *J. Hydro-environ. Res.*, *6*(4), 275–285.
Zeinstra-Helfrich, M., W. Koops, and A. J. Murk (2015), The NET effect of dispersants—A critical review of testing and modelling of surface oil dispersion, *Mar. Pollut. Bull.*, *100*(1), 102–111.
Zelenke, B., C. O'Connor, C. Barker, C. J. Beegle-Krause, and L. Eclipse (2012), General NOAA Operational Modeling Environment (GNOME) Technical Documentation, report, 105 pp., Emergency Response Div., NOAA, Seattle, Wash.
Zhao, L., M. C. Boufadel, S. A. Socolofsky, E. Adams, T. King, and K. Lee (2014), Evolution of droplets in subsea oil and gas blowouts: Development and validation of the numerical model VDROP-J, *Mar. Pollut. Bull.*, *83*(1), 58–69.
Zheng, L., and P. Yapa (2000), Buoyant velocity of spherical and nonspherical bubbles/droplets, *J. Hydraul. Eng.*, *126*, 852–854.
Zheng, L., P. D. Yapa, and F. H. Chen (2003), A model for simulating deepwater oil and gas blowouts–Part I: Theory and model formulation, *J. Hydraul. Res.*, *41*(4), 339–351.